THE JOURNAL OF BIOLOGICAL CHEMISTRY VOL. 281, NO. 3, pp. 1580–1586, January 20, 2006

Human TRPV4 Channel Splice Variants Revealed a Key Role of Ankyrin Domains in Multimerization and Trafficking*

Received for publication, October 21, 2005, and in revised form, November 2, 2005 Published, JBC Papers in Press, November 16, 2005, DOI 10.1074/jbc.M511456200

Maite Arniges[‡], José M. Fernández-Fernández[‡1], Nadine Albrecht[§], Michael Schaefer[§], and Miguel A. Valverde[‡2]

From the [‡]Grup de Canalopaties, Unitat de Senyalització Cellular, Universitat Pompeu Fabra, C/Dr. Aiguader 80, 08003 Barcelona, Spain and the [§]Institut für Pharmakologie, Campus Benjamin Franklin, Charité, Universitätsmedizin Berlin, Thielallee 63-73, 14195 Berlin, Germany

The TRPV4 cation channel exhibits a topology consisting of six predicted transmembrane domains (TM) with a putative pore loop between TM5 and TM6 and intracellular N- and C-tails, the former containing at least three ankyrin domains. Functional transient receptor potential (TRP) channels are supposed to result following the assembly of four subunits. However, the rules governing subunit assembly and protein domains implied in this process are only starting to emerge. The ankyrin, TM, and the C-tail domains have been identified as important determinants of the oligomerization process. We now describe the maturation and oligomerization of five splice variants of the TRPV4 channel. The already known TRPV4-A and TRPV4-B (Δ384–444) variants and the new TRPV4-C (Δ237–284), TRPV4-D (Δ27–61), and TRPV4-E (Δ237–284 and Δ384–444) variants. All alternative spliced variants involved deletions in the cytoplasmic N-terminal region, affecting (except for TRPV4-D) the ankyrin domains. Subcellular localization, fluorescence resonance energy transfer, co-immunoprecipitation, glycosylation profile, and functional analysis of these variants permitted us to group them into two classes: group I (TRPV4-A and TRPV4-D) and group II (TRPV4-B, TRPV4-C, and TRPV4-E). Group I, unlike group II variants, were correctly processed, homo- and heteromultimerized in the endoplasmic reticulum, and were targeted to the plasma membrane where they responded to typical TRPV4 stimuli. Our results suggest that: 1) TRPV4 biogenesis involves core glycosylation and oligomerization in the endoplasmic reticulum followed by transfer to the Golgi apparatus for subsequent maturation; 2) ankyrin domains are necessary for oligomerization of TRPV4; and 3) lack of TRPV4 oligomerization determines its accumulation in the endoplasmic reticulum.

The non-selective cation channel TRPV4 is a member of the transient receptor potential (TRP)[3] family of channels (1). TRPV4 shows multiple modes of activation and regulatory sites, enabling it to respond to various stimuli, including osmotic cell swelling (2–5), mechanical stress (6–8), heat (9), acidic pH (7), endogenous ligands (10), high viscous solutions (11), and synthetic agonists such as 4α-phorbol 12,13-didecanoate (4α-PDD) (12). TRPV4 mRNA is expressed in a broad range of tissues (13), although functional tests have only been carried out in a few: endothelial (14), epithelial (5, 11, 15), smooth muscle (16), keratinocytes (17), and DRG neurons (18). An alternative splice variant lacking the seventh exon has also been cloned from human aortic endothelial cells (19), although this variant was not further investigated because of its unresponsiveness to hypotonic stimuli.

The general topology of a TRP subunit consists of six predicted transmembrane domains (TM) with a putative pore loop between TM5 and TM6 and intracellular N- and C-terminal regions of variable length, the former containing multiple ankyrin (ANK) repeats in the TRPC, TRPA, TRPN, and TRPV subfamilies (1). ANK repeats are modular protein interaction domains, each composed by ≈33 amino acids with a highly conserved secondary structure of helix turn helix that determines its interaction properties (20). Functional TRP channels are supposed to result following the assembly of four TRP subunits. Although multimerization has been already demonstrated for various members of the TRP family (including TRPV4) (21–25), the tetrameric structure has only been proposed for a few TRP channels (26–28).

The rules governing subunit assembly and the protein domains implied in this oligomerization process are just starting to emerge (29, 30). Several studies suggest the participation of the cytosolic N-terminal region in the assembly of homo- or heteromultimeric TRP channels (23, 31, 32), and two recent papers narrowed down the role of the ANK domains in the oligomerization process of TRPV5 and TRPV6 channels (24, 33). On the other hand, transmembrane domains (25) and the cytoplasmic C terminus (34) have also been identified as important determinants of the oligomerization process of TRPV channels.

In this study we characterized the oligomerization, maturation, localization, and ion channel function of five splice variants of the TRPV4 channel. Variants lacking part of the ANK domains did not oligomerize, were retained in the ER, and did not produce functional channels at the plasma membrane.

EXPERIMENTAL PROCEDURES

Cloning and Mutagenesis of Human TRPV4—TRPV4 splice variants were cloned from the human tracheal epithelial cell line CFT1-LCFSN using the reverse transcriptase-PCR protocol previously described (5). cDNAs were sequenced and subcloned into the pcDNA3.1, pcDNA3-FLAG, pcDNA3-YFP, and pcDNA3-CFP vectors (Invitrogen). For the generation of the C-terminal fusion proteins and mutagenesis of the R*X*R motifs we used the QuikChange Mutagenesis Kit (Stratagene). The first arginine of each of the four RXR domains ([122]RWR, [269]RGR, [816]RLR, and [819]RDR) in TRPV4 channels was mutated to alanine using the following primers: forward primers, 5′-CTCCAGTGACAACAAGGCGTGGAGGAAGAAGATCATAG-3′, 5′-ATGTCCACGCCCAGGCCGCTGGGCGCTTCTTCCAGC-3′, 5′-TTCTCGCATACCGTGGGCGCCCTCCGCAGGGATCGCT-3′, 5′-TGGGCC-

* This work was supported in part by Spanish Ministry of Science and Technology Grant SAF2003–1240, red HERACLES (FIS), and Generalitat de Catalunya Grant SGR05–266. The costs of publication of this article were defrayed in part by the payment of page charges. This article must therefore be hereby marked "*advertisement*" in accordance with 18 U.S.C. Section 1734 solely to indicate this fact.

[1] Ramon y Cajal Fellow.

[2] To whom correspondence should be addressed: C/Dr. Aiguader 80, Barcelona 08003, Spain. Tel.: 34-93-542-2832; Fax: 34-93-542-2802; E-mail: miguel.valverde@upf.edu.

[3] The abbreviations used are: TRP, transient receptor potential; 4α-PDD, 4α-phorbol 12,13-didecanoate; ANK, ankyrin domain; ERGIC, endoplasmic reticulum/Golgi intermediate compartment; FRET, fluorescence resonance energy transfer; TM, transmembrane domains; ER, endoplasmic reticulum; YFP, yellow fluorescent protein; CYP, cyan fluorescent protein; PNGase F, *N*-glycosidase F; Endo H, endoglycosidase H.

GCCTCCGCGCGGATCGCTGGTCCT-3′ and the corresponding reverse primers.

Cell Culture and Transient Transfection—CFT1-LCFSN human tracheal epithelial cells, HEK-293, and HeLa cells were grown as previously described (5, 11). Fluorescent resonance energy transfer (FRET) was carried out on HEK-293 cells transfected with 0.4 μg of CFP-tagged TRPV4 channel isoform and 1.6 μg of YFP-tagged subunit using FuGENE 6 transfection reagent (Roche). For coimmunoprecipitation experiments HEK-293 cells were grown in 60-mm dishes and transfected with 2 μg of FLAG- and 2 μg of YFP-tagged plasmids. Immunofluorescence, glycosylation, and functional studies were carried out on HeLa cells transfected with ExGen500 (Fermentas MBI). 3 μg of the TRPV4 constructs and 7 equivalents of polyethylenimine, together with the transfection reporter pEGFP-N1 (for functional studies) at a 10:1 ratio, were added to each 35-mm dish.

Confocal Microscopy—Cells transiently transfected with pcDNA3.1 or pcDNA-YFP constructs were probed with a polyclonal affinity purified anti-human TRPV4 (1:1000) (5, 11), mouse anti-calnexin and GM130 (1:50 and 1:1000, respectively; BD Biosciences), and α-ER-GIC-53 (1:1000) monoclonal antibodies (a gift from R. Hermosilla, Charité-Universitätsmedizin Berlin). Alexa Fluor 595 goat anti-rabbit or Alexa 633 goat anti-mouse (Molecular Probes, 1:3000 and 1:1000, respectively) were used as secondary antibodies. Digital images were taken and analyzed using a Leica TCS SP or Carl Zeiss LSM 510-META confocal microscopes as previously described (25).

Deglycosylation with PNGase F and Endo H—Total protein was extracted from HeLa cells 24 h after transfection. Cells were lysed in a buffer containing (mM): 150 NaCl, 5 EDTA, 1% Nonidet P-40, 1 sodium orthovanadate, 1 phenylmethylsulfonyl fluoride, 0.05% aprotinin, and 1 dithiothreitol (1 h at 4 °C). The lysis buffer was supplemented with a Complete Mini protease inhibitor mixture (1:7, v/v; Roche). The nuclear fraction was pelleted by centrifugation at 12,000 × *g* for 15 min. 20 μg of total protein were digested with 2 μl of Endo H or PNGase F (New England Biolabs) for 1.5 h at 37 °C following the manufacturers instructions. Proteins were subjected to SDS-PAGE (8%) and subsequently electroblotted onto nitrocellulose membranes. Incubation with anti-human TRPV4 antibody (1:500) for 1 h at room temperature was followed by incubation for 1 h at room temperature with the horseradish peroxidase-conjugated donkey anti-rabbit IgG (Amersham Biosciences) at a dilution of 1:2000. Detection was done with a SuperSignal West chemiluminescent substrate (Pierce).

FRET and Coimmunoprecipitation—FRET measurements were carried out in a monochromator equipped with a digital video imaging system (TILL-Photonics, Germany) attached to an inverted epifluorescence microscope (Axiovert 100, Carl Zeiss). Experiments were performed in a HEPES-buffered solution containing (mM): 138 NaCl, 6 KCl, 1 HEPES, 1 $MgCl_2$, 1 $CaCl_2$, 5.5 glucose, 2 mg/ml bovine serum albumin, and 10 HEPES, pH 7.4. Single-cell FRET efficiencies were obtained after monitoring the increase in the CFP (FRET-donor) fluorescence emission during selective YFP (FRET-acceptor) photobleaching (25, 35). FRET efficiency was expressed as the mean ± S.E. of a set of 6–15 experiments with more than 6 cells/experiment. Coimmunoprecipitation experiments were carried out following the protocol described previously (25) using anti-FLAG M2 monoclonal antibody (Sigma) for immunoprecipitation and anti-FLAG M2 or 1:1000 polyclonal rabbit anti-GFP (Clontech) antibodies for immunodetection.

Cytosolic Ca^{2+} Measurements—Changes in the intracellular Ca^{2+} concentration were measured in cells loaded with 5 μM fura 2-AM (Molecular Probes) incubated for 30 min at 37 °C followed by de-esterification for 15 min at room temperature. The ratio of emitted fluorescence (510 nm) following alternating excitation at 340 and 380 nm was obtained as previously described (15). The isotonic bathing solution contained (mM): 2.5 KCl, 140 NaCl, 1.2 $CaCl_2$, 0.5 $MgCl_2$, 5 glucose, 10 HEPES (310 mosmol/liter, pH 7.35). The hypotonic bathing solution (220 mosmol/liter, pH 7.35) was prepared by omitting 50 mM NaCl from the isotonic Hanks' solution and osmolality was adjusted with D-mannitol when necessary. Results are expressed as mean ± S.E. of *n* observations.

Electrophysiological Recordings—Single-channel currents were recorded from HEK-293-transfected cells at different voltage (ranging from −100 to +100 mV) in the inside-out patch clamp mode (36). The pClamp8 software (Axon Instruments, Foster City, CA) was used for pulse generation, data acquisition through an Axon Digidata A/D interface, and subsequent analysis. Borosilicate glass patch pipettes had 5–10 megaohm resistance and were filled with a solution containing (mM): 125 NaCl, 1.5 $MgCl_2$, 1 EGTA, and 10 HEPES (300 mosmol/liter, pH 7.35). The bath solution was (mM) 130 CsCl, 1 $MgCl_2$, 1 Na_2ATP, 0.034 $CaCl_2$, 5 EGTA, 10 HEPES (310 mosmol/liter, pH 7.25). Currents were acquired at 5 KHz and low-pass filtered at 1 kHz. Experiments were performed at room temperature (22–26 °C). Channel activity of both TRPV4-A and TRPV-D isoforms was assessed as the NPo (number of channels × single channel open probability) from 15-s continuous recordings before and after the addition of 4α-PDD.

RESULTS

Cloning of TRPV4 Variants from Human Airway Epithelial Cells—A reverse transcriptase-PCR-based cloning process identified 5 variants of the TRPV4 channel in human tracheal epithelial cells. Two of the cloned cDNAs corresponded to the already described TRPV4 isoform A (full-length cDNA; GenBank® number NM_021625) and TRPV4 isoform B (lacking exon number 7, number NM_147204; Δ384–444 amino acids). Variant B was originally described as an isoform lacking exon 6 (number AB073669), although subsequent analysis of the genomic structure of the *TRPV4* gene identified a further 5′ non-coding exon 1, therefore renumbering the TRPV4 exons. We also identified three new splice variants, named TRPV4-C, TRPV4-D, and TRPV4-E variants (Fig. 1*A*), affecting the cytoplasmic N-terminal region. TRPV4-C lacks exon 5 (number DQ59644; Δ237–284 amino acids), TRPV4-D presents a short deletion inside exon 2 (number DQ59645; Δ27–61 amino acids), and TRPV4-E (number DQ59646; Δ237–284 and Δ384–444 amino acids) is produced by a double alternative splicing lacking exons 5 and 7. Splicing sites for the TRPV4-D variant are given by two canonical dinucleotides, GT and AG for donor and acceptor sites, respectively. All variants cloned contained the synonymous single nucleotide polymorphism in position 761 (dbSNP reference number rs3825394). Transcripts for these five variants have been also amplified from the human bronchial epithelial cell line HBE (results not shown).

Functional Measurements of the Human TRPV4 Variants—The TRPV4-A channel responds to a wide variety of stimuli (13). To functionally evaluate TRPV4 variants we transiently transfected HeLa cells and measured intracellular Ca^{2+} concentration ($[Ca^{2+}]_i$) in response to three different well known activators of TRPV4 (Fig. 1). As a negative control, HeLa cells were transfected with the backbone plasmid (Fig. 1, *B–D*). 30% Hypotonicity, 1 μM 4α-PDD, and 10 μM arachidonic acid induced increases in $[Ca^{2+}]_i$ for TRPV4-A (■) and TRPV4-D channels (*light grey square*) (Fig. 1, *E–G*), whereas no response was observed for TRPV4-B (▲), TRPV4-C (*light grey triangle*), and TRPV4-E (*dark grey triangle*) transfected cells (Fig. 1, *H–J*). No apparent differences in the Ca^{2+} response were seen between TRPV4-A and TRPV4-D variants.

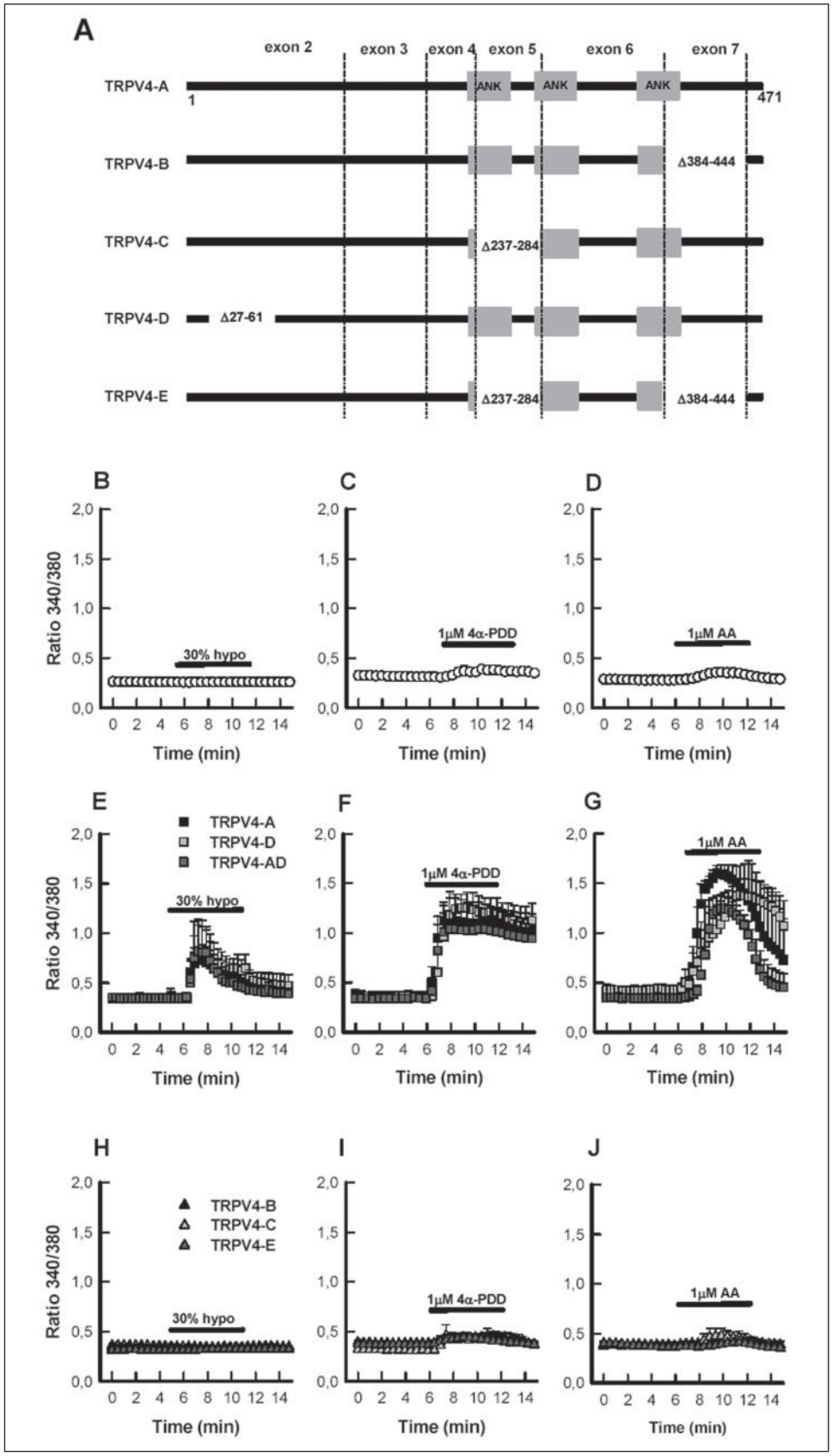

FIGURE 1. **Identification and function of TRPV4 variants in human airway epithelial cells.** *A*, schematic diagram showing the intracellular N-terminal region of the human TRPV4 channel (amino acids 1–471). Exons and the corresponding amino acids lost in each TRPV4 isoform are indicated by *numbers*. *B–J*, functional analysis of TRPV4 variants. Fura-2 ratios obtained in control HeLa cells transfected with the empty vector pEGFP-C1 (*B–D*), TRPV4-A and -D (*E–G*), TRPV4-B, -C, and -E (*H–J*), and stimulated with 30% hypotonic solution, 1 μM 4α-PDD, or 10 μM arachidonic acid. Traces are mean ± S.E. of 10–20 cells measured in three to four independent experiments.

Excised inside-out electrophysiological analysis of TRPV4-A and TRPV4-D expressing HEK-293 cells (Fig. 2) showed spontaneous single channel activity (NPo, measured at +100 mV), which was equally increased by the application of 1 μM 4α-PDD (from 0.049 ± 0.02 to 0.91 ± 0.05; $n = 17$ in TRPV4-A transfected cells, and from 0.05 ± 0.039 to 0.91 ± 0.08; $n = 9$ in TRPV4-D transfected cells). No differences in

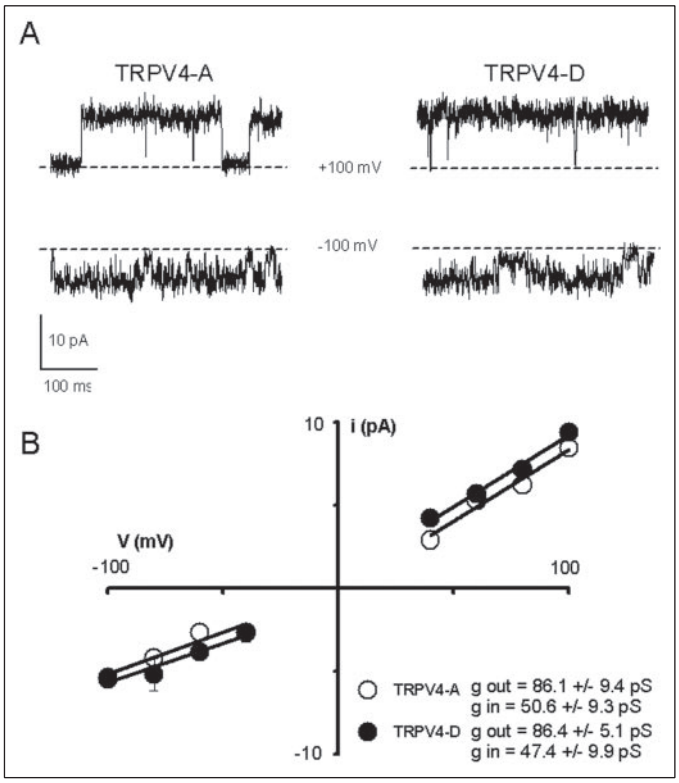

FIGURE 2. **TRPV4-A and TRPV4-D isoforms produce functional channels with similar properties when expressed in HEK-293 cells.** *A*, current traces obtained from TRPV4-A- and TRPV4-D-expressing HEK-293 cells at the indicated voltages in the presence of 1 μM 4α-PDD. *Dashed lines* indicate the zero current level. *B*, I–V relationship of 4α-PDD-activated TRPV4-A (*open circle*) and TRPV4-D (*closed circle*) channels in inside-out patches.

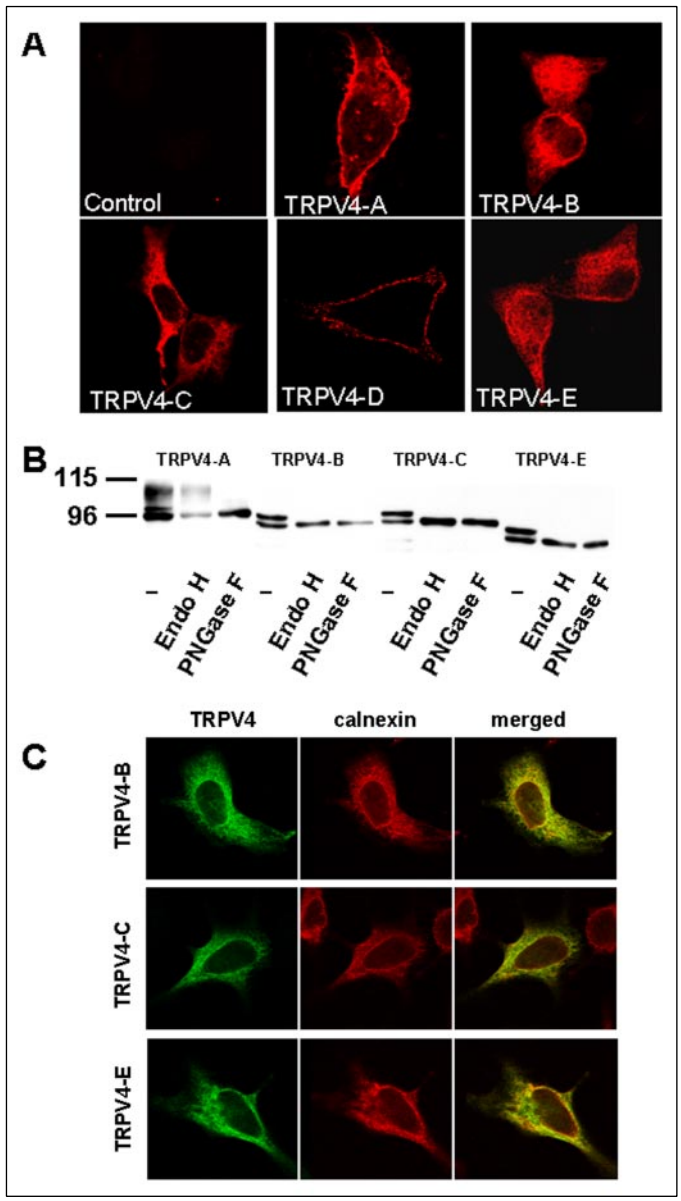

FIGURE 3. **Expression and subcellular localization of TRPV4 variants.** *A*, immunolocalization of TRPV4 isoforms in transiently transfected HeLa cells. Confocal microscopy images obtained after immunostaining with a polyclonal anti-human TRPV4 antibody. *B*, glycosylation analysis of TRPV4 variants. Total protein (20 μg) from transiently transfected HeLa cells was isolated and treated with Endo H (*EH*) or PNGase F (*PF*) or untreated (−). *C*, colocalization of TRPV4-B, TRPV4-C, and TRPV4-E variants (*left panels*, *green*) expressed in HeLa cells with the ER marker calnexin (*middle panels*, *red*). Merged images (*right panels*) show extensive colocalization of TRPV4 type II variants and the ER marker.

inward and outward single-channel slope conductances were also observed between TRPV4-A (50.6 ± 9.3 pS (n = 7) and 86.1 ± 9.4 pS (n = 17)) and TRPV4-D isoforms (47.4 ± 9.9 pS (n = 5) and 86.4 ± 5.1 pS (n = 9)). Single-channel events did not appear in HEK-293 control cells transfected with pEGFP only, either in the absence or presence of 4α-PDD (n = 10).

Expression and Subcellular Localization of TRPV4 Channel Variants—Immunolocalization of TRPV4 variants was carried out on transiently transfected HeLa cells with an antibody raised against TRPV4 (5, 11). Fig. 3*A* shows that TRPV4-A and TRPV4-D proteins displayed a robust cell surface expression, whereas TRPV4-B, TRPV4-C, and TRPV4-E proteins showed a reticular intracellular immunostaining, indicative of retention in the ER.

To determine whether B, C, and E variants were trapped in the ER, we analyzed their glycosylation profile and carried out colocalization studies with calnexin (an ER resident protein) in transfected HeLa cells. Total cell protein was treated with Endo H to remove *N*-linked high mannose glycosylations (indicative of ER forms) or PNGase F to remove both high mannose and complex glycosylation (indicative of post-ER forms). TRPV4-A was used as a control. As shown in Fig. 3*B*, three immunoreactive protein bands with apparent molecular masses of 96, 100, and 110 kDa were detected for TRPV4-A (and TRPV4-D, results not shown) in untreated samples. The 96-kDa band represents the non-glycosylated form of the TRPV4-A. The 100-kDa band, but not the 110-kDa band, was sensitive to Endo H and both bands were sensitive to PNGase F. Thus the 100-kDa band represents the high mannose and the 110-kDa band the complex glycosylated form. An identical glycosylation pattern was observed for the TRPV4-D isoform (results not shown). An identical glycosylation pattern and Endo H/PNGase F sensitivity was observed for the TRPV4-D isoform (results not shown). In contrast, the TRPC4-B, -C, and -E variants gave rise to two immunoreactive bands migrating at 91 and 96 kDa, 92 and 97 kDa, and 86 and 90 kDa, respectively. The *upper band* disappeared upon treatment with Endo H or PNGase F (Fig. 3*B*) indicating the presence of high-mannose glycosylation, but a lack of further maturation. *O*-Glycosylation of TRPV4-A can be excluded because PNGase F treatment produces a unique band with an apparent molecular weight corresponding to the predicted size of the non-glycosylated protein. Taken together, the data suggest that B, C, and E variants are retained in the ER, whereas TRPV4-A and TRPV4-D are fully processed and reach the plasma membrane where they produce functional channels. Confirmation of ER retention for B, C, and E variants was obtained by colocalization

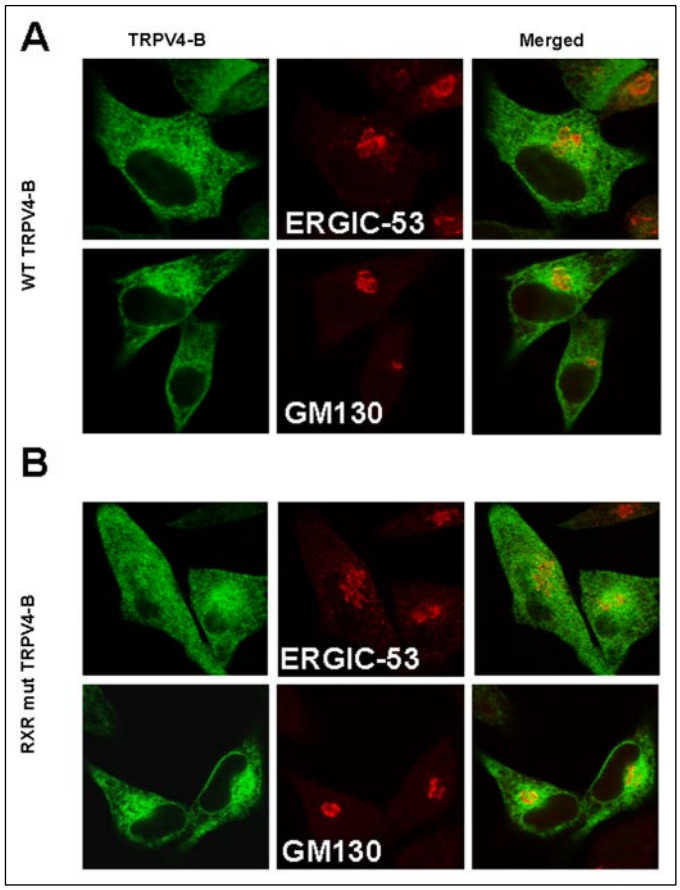

FIGURE 4. **Lack of TRPV4-B colocalization to ERGIC or Golgi.** *A*, TRPV4-YFP fluorescence detection in transfected HeLa cells (*green*), co-stained with ERGIC and Golgi markers ERGIC-53 and GM130 (in *red*) and channel overlay. *B*, fluorescence detection of R*X*R-mutated TRPV4-YFP (*green channel*) and counterstaining with ERGIC and Golgi markers (*red channel*). Absence of colocalization is apparent in merged images (*right panels*) obtained from both wild-type and mutant TRPV4-B.

studies. All three variants overlap with the ER resident chaperone calnexin (Fig. 3*C*). No colocalization of TRPV4-B variant with the ER/Golgi intermediate compartment (ERGIC) or the Golgi markers, αERGIC-53 and GM130, respectively, was detected (Fig. 4*A*). Identical results were obtained with TRPV4-C and -E (not shown).

Homomerization of TRPV4 Variants—Functional TRP channel complexes require the tetrameric assembly of pore-forming subunits (30). Therefore, quality control mechanisms must be met to ensure the correct quaternary structure. Several compartments, including ER and the Golgi, have been identified as sites for oligomerization (37, 38). Thus, we next checked the multimerization of the TRPV4 variants. For this purpose, we evaluated the proximity of CFP- and YFP-tagged TRPV4 variants, as an indication of subunit assembly by FRET technique (25). The relative CFP and YFP fluorescence intensities were determined for every single cell to ensure comparable levels of TRPV4 expression and to adjust the 1.5–3-fold molar ratio between acceptor- (YFP) and donor (CFP)-labeled subunits. Fig. 5 shows FRET efficiencies obtained in HEK-293 cells transiently co-transfected with expression plasmids encoding CFP- or YFP-fused TRPV4 isoforms. TRPV4-A and TRPV4-D variants displayed a higher FRET efficiency (17.5 ± 0.94 and 18.32 ± 1.07, respectively) compared with TRPV4-B, TRPV4-C, and TRPV4-D (around 5%). FRET results indicate that only TRPV4-A and TRPV4-D efficiently assemble into homomeric channel complexes.

To check whether TRPV4 channels oligomerize in the ER we carried out FRET analysis of HeLa cells transfected with CFP- and YFP-fused

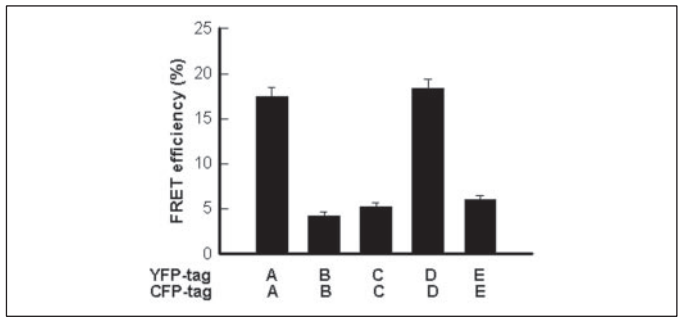

FIGURE 5. **Homomerization of TRPV4 variants.** FRET efficiencies determined between identical CFP- and YFP-fused TRPV4 variants (*A–E*) transiently cotransfected in HEK-293 cells. High FRET efficiencies corresponding to homomultimer formation could only be demonstrated for TRPV4-A and TRPV4-D variants.

TRPV4-A variants and treated for 10 h after transfection with the intracellular transport inhibitor brefeldin A (0.5 μg/liter), which prevents transport from the ER to the Golgi (39). FRET efficiencies (measured 14 h after transfection) for homomeric TRPV4-A were not statistically different between solvent-treated and brefeldin A-treated cells (24.1 ± 1.3 and 19.4 ± 3.3%, respectively; $n = 3$; $p > 0.05$). This result suggests that assembly of TRV4 occurs primarily in the ER and that ER sequestration of TRPV4-B, -C, and -E variants is related to their inability to oligomerize in the ER.

One possible mechanism explaining the intracellular sequestration of channel subunits involves the participation of bi-arginine (R*X*R) retention motifs, which are hidden under the tetrameric structure but when exposed in non-assembled channel subunits determine their intracellular retention (40). TRPV4 protein contains 4 R*X*R motifs, two on the N-terminal (^{122}RWR and ^{269}RGR) and two on the C-terminal (^{816}RLR and ^{819}RDR) intracellular tails. Expression of TRPV4-B variants containing alanine mutations in the first arginine of either of the four R*X*R motifs did not modify the localization of TRPV4-B (data not shown). Likewise, a TRPV4-B construct in which all four R*X*R motifs were modified by alanine mutations was still retained in the ER and did not migrate to the ERGIC or Golgi (Fig. 4*B*).

Heteromerization of TRPV4 Variants—Heteromeric assembly of TRP channels can produce a change in the intracellular localization and/or modify the function of the new assembled protein (33, 41, 42). To test whether TRPV4-A could rescue TRPV4-B, TRPV4-C, and TRPV4-E isoforms retained in the ER, we co-expressed TRPV4-A-YFP and CFP-fused variants in HEK-293 cells and visualized the subcellular distribution by confocal laser microscopy. As shown in Fig. 6*A* plasma membrane overlapping was only observed in cells expressing TRPV4-A and TRPV4-D (with almost identical localization), whereas partial overlap in intracellular compartments was detected for all combinations of TRPV4 variants. It is also worth noting the apparent lack of redistribution to the plasma membrane of the intracellular variants (B, C, and E) following coexpression with the YFP-tagged TRPV4-A isoform. TRPV4-B, TRPV4-C, and TRPV4-E proteins failed to reach the plasma membrane even if coexpressed with excess amounts of targeting competent TRPV4-A-YFP.

Heteromerization of TRPV4 variants was also tested by FRET and coimmunoprecipitation analysis. Using TRPV4-A-YFP as the FRET-acceptor and CFP-fused TRPV4-B-E variants as donors, a high FRET efficency of 21.7 ± 3.5 could only be demonstrated for the heteromeric channel formation between TRPV4-A and TRPV4-D subunits. By contrast, FRET efficiencies remained low for TRPV4-A coexpressed with TRPV4-B, TRPV4-C, or TRPV4-E (Fig. 6*B*). Heteromeric TRP proteins may modify the response of the resulting channel compared with the homomeric channel, a possibility we also evaluated. Measurements of $[Ca^{2+}]_i$ in cells expressing heteromultimeric TRPV4-A/TRPV4-D channels did not differ from the homomultimeric TRPV4-A and

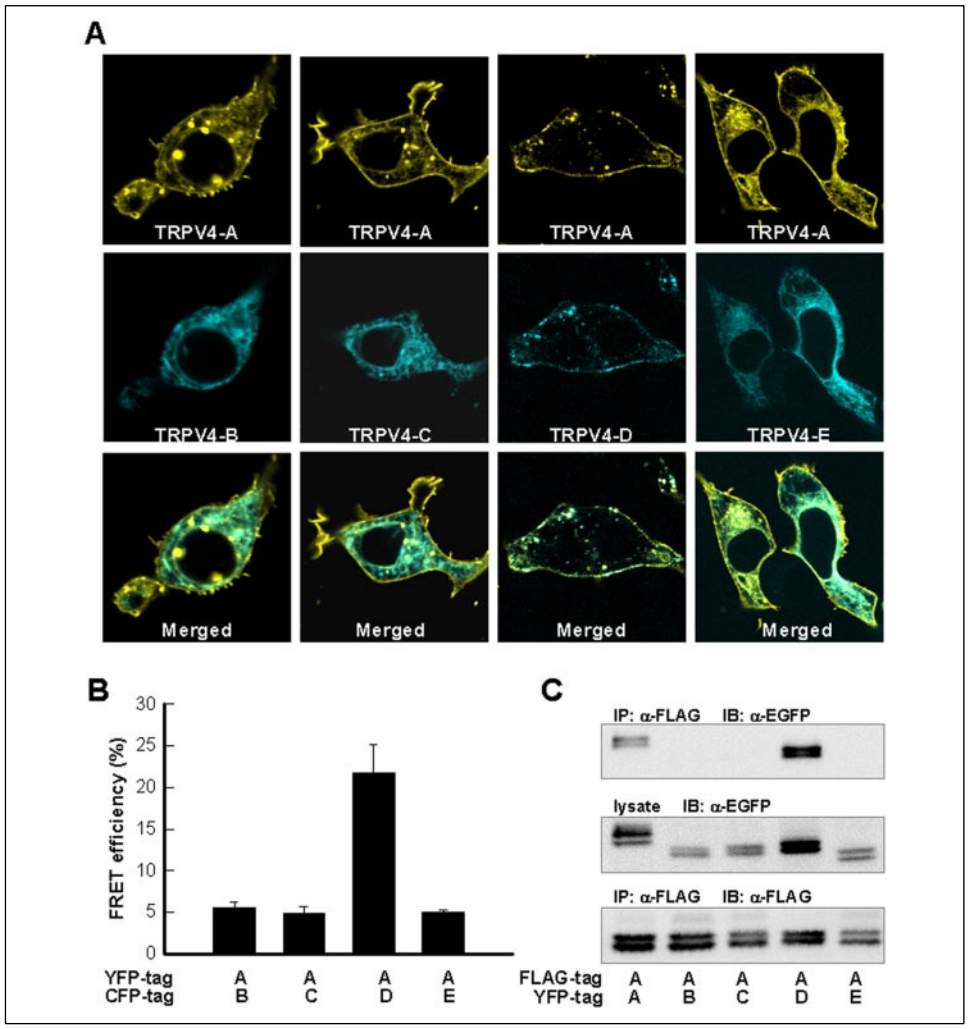

FIGURE 6. **Heteromerization of TRPV4 variants.** *A*, different combinations of TRPV4 channels tagged with YFP (*TRPV4-A*) or CFP (*TRPV4-B–E*) were coexpressed in HEK-293 cells and imaged by confocal microscopy. Colocalization at the plasma membrane only exists for the coexpressed TRPV4-A-YFP and TRPV4-D-CFP subunits. *B*, FRET efficiencies determined between different TRPV4 variants showed heterooligomerization only for A and D proteins ($n = 6$). *C*, coimmunoprecipitation of coexpressed TRPV4 channel subunits. Plasmids encoding TRPV4 channels C-terminal tagged with FLAG or YFP were cotransfected in HEK-293 cells. TRPV4 isoforms in the membrane lysates (*middle panel*) and co-immunoprecipitated subunits (*upper panel*) were detected by immunoblotting (*IB*) with α-GFP antibodies. The *lower panel* shows the recovery of immunoprecipitated TRPV4-A-FLAG.

TRPV4-D channels (Fig. 1, *E–G*) probed with 30% hypotonicity, 1 μM 4α-PDD, and 10 μM arachidonic acid.

Coimmunoprecipitation experiments confirmed the FRET data. From all the combinations tested with the TRPV4-A-FLAG-tagged protein coexpressed with TRPV4-YFP isoforms in HEK-293 cells, we were able to coimmunoprecipitate only the TRPV4-D variant (Fig. 6*C*, *top panel*). Lysate was probed with anti-YFP antibody (Fig. 6*C*, *middle panel*), to check the expression of the transfected YFP variants, and the immunoprecipitates with anti-FLAG antibody (Fig. 6*C*, *lower panel*), proving the recovery of the FLAG protein, are also shown. No FRET or coimmunoprecipitation between TRPV4-B, -C, and -E variants was detected (results not shown).

DISCUSSION

Our study of oligomerization, localization, and channel activity of human TRPV4 splice variants has allowed us to identify the N-terminal ANK repeats as key molecular determinants of subunit assembly and subsequent processing of the assembled channel. Using a combined approach of several independent methods we have described five TRPV4 variants (TRPV4-A–E) cloned from human airway epithelial cells, three of which were described for the first time (TRPV4-C–E). We have grouped them into two classes: group I (including TRPV4-A and TRPV4-D) and group II (including TRPV4-B, TRPV4-C, and TRPV4-E). Group I variants are correctly processed and targeted to the plasma membrane where they form functional channels with similar electrophysiological properties. Variants from group II, which are lacking parts of the ANK domains are unable to oligomerize and were retained intracellularly, in the ER.

Misfolded channel proteins and/or oligomerization-deficient subunits can be identified and intracellularly retained by quality control mechanisms in the ER (37, 43). Therefore, it is particularly important to identify the structural domains involved in the oligomerization process. In the case of TRP channels, identification of the assembly pathway is starting to emerge (30). The N-tail of TRP channels, as it occurs for voltage-gated K^+ channels (33), has also been identified as a possible multimerization domain (23–25, 31–33). In the case of TRPV5 and TRPV6 a key oligomerization domain has been narrowed down to the N-terminal ANK domains (24, 33). C-tails and transmembrane domains have also been suggested to participate in the oligomerization and/or stabilization of assembled TRP channels (33, 34), including TRPV4 (25).

Our study of TRPV4-B, -C, and -E splice variants (missing part of the ANK domains) by *in vivo* FRET and coimmunoprecipitation methods has allowed us to show for the first time three important traits of TRPV4 biogenesis. 1) Glycosylation of TRPV4 channel involves ER to Golgi transport with the corresponding change in the *N*-linked oligosaccharides from the high mannose type characteristic of the ER to the complex type characteristic of the Golgi apparatus, without apparent *O*-glycosylation. 2) TRPV4-A subunits oligomerize in the ER (no significant differences in FRET efficiency were seen in the absence or presence of brefeldin A, an inhibitor of ER to Golgi transport). 3) Impaired subunit assembly of type II variants is because of the lack of N-terminal ANK domains and causes protein retention in the ER. Although we propose that ER retention of TRPV-B, -C, and E variants is directly related to

their inability to oligomerize we cannot unequivocally discard that such retention is because of protein misfolding.

Subunit misfolding is a cause of inefficient ion channel assembly, but folding events of ion channel subunits also occur after subunit assembly, *i.e.* subunits oligomerize even if their folding is not complete (37, 44). A possible mechanism for ER retention of unoligomerized subunits involves exposure of a retention signal sequence (R*X*R), which otherwise is shielded in completely assembled channels (40, 45). R*X*R motifs play a role in monitoring the assembly of multimeric proteins and TRPV4 presents four R*X*R motifs, two in each intracellular tails. However, mutation of all R*X*R motifs did not modify the intracellular distribution of type II variants, similarly to what have been reported for other membrane proteins (46). The implication of other ER-transport signals (47, 48) in the retention of type II TRPV4 variants is a mechanism that remains to be addressed.

Intriguingly, an early study on truncated rat TRPV4 lacking the three ANK domains reported a delayed response to hypotonicity (3). At present, we cannot explain how these truncated proteins, which according to our results should not oligomerize, can produce functional channels. Certainly, the original observation by Liedtke and colleagues (3) should be re-evaluated in view of our results and those of others demonstrating impaired function of TRPV4 (49) and TRPV6 (24) channels with deleted ANK domains.

Ion channel functional diversity is greatly enlarged by both the presence of splice variants and heteromerization of different pore-forming and regulatory subunits. Alternative splicing is a major contributor to protein diversity (50). Within the TRP family of ion channels several splice variants have been identified, some of them resulting in lack of responses to typical stimuli, others modifying the pore properties, and those exerting dominant negative effects (42, 51–54). Group II TRPV4 splice variants have been identified in two unrelated, human airway epithelial cell lines (CFT1-LCFSN and HBE). Considering the relevance of TRPV4 channels in epithelial physiology (5, 11, 55), it may be conceivable that a change in the expressed ratio of group I to group II variants, favoring the later, would modify normal epithelial functioning. Splicing can be regulated by several stressing stimuli (56) including pH, osmotic, and temperature shocks, all of them being also activating stimuli of the TRPV4. Therefore, it will be interesting to test whether such stimuli modify the expressed ratio of TRPV4 group I to group II variants.

Acknowledgments—We thank E. Vázquez, Y. Andrade, and J. Fernandes for valuable discussions; Y. Tor for technical support; and I. Uribesalgo and G. Cantero for help at some stages of this work.

REFERENCES

1. Montell, C. (2005) *Sci. STKE 2005*, re3
2. Strotmann, R., Harteneck, C., Nunnenmacher, K., Schultz, G. & Plant, T. D. (2000) *Nat. Cell. Biol.* **2,** 695–702
3. Liedtke, W., Choe, Y., Marti-Renom, M. A., Bell, A. M., Denis, C. S., Sali, A., Hudspeth, A. J., Friedman, J. M. & Heller, S. (2000) *Cell* **103,** 525–535
4. Wissenbach, U., Bodding, M., Freichel, M. & Flockerzi, V. (2000) *FEBS Lett.* **485,** 127–134
5. Arniges, M., Vazquez, E., Fernandez-Fernandez, J. M. & Valverde, M. A. (2004) *J. Biol. Chem.* **279,** 54062–54068
6. Gao, X., Wu, L. & O'Neil, R. G. (2003) *J. Biol. Chem.* **278,** 27129–27137
7. Suzuki, M., Mizuno, A., Kodaira, K. & Imai, M. (2003) *J. Biol. Chem.* **278,** 22664–22668
8. Liedtke, W., Tobin, D. M., Bargmann, C. I. & Friedman, J. M. (2003) *Proc. Natl. Acad. Sci. U. S. A.* **100,** Suppl. 2, 14531–14536
9. Guler, A. D., Lee, H., Iida, T., Shimizu, I., Tominaga, M. & Caterina, M. (2002) *J. Neurosci.* **22,** 6408–6414
10. Watanabe, H., Vriens, J., Prenen, J., Droogmans, G., Voets, T. & Nilius, B. (2003) *Nature* **424,** 434–438
11. Andrade, Y. N., Fernandes, J., Vazquez, E., Fernandez-Fernandez, J. M., Arniges, M., Sanchez, T. M., Villalon, M. & Valverde, M. A. (2005) *J. Cell Biol.* **168,** 869–874
12. Watanabe, H., Davis, J. B., Smart, D., Jerman, J. C., Smith, G. D., Hayes, P., Vriens, J., Cairns, W., Wissenbach, U., Prenen, J., Flockerzi, V., Droogmans, G., Benham, C. D. & Nilius, B. (2002) *J. Biol. Chem.* **277,** 13569–13577
13. Nilius, B., Vriens, J., Prenen, J., Droogmans, G. & Voets, T. (2004) *Am. J. Physiol.* **286,** C195–C205
14. Vriens, J., Owsianik, G., Fisslthaler, B., Suzuki, M., Janssens, A., Voets, T., Morisseau, C., Hammock, B. D., Fleming, I., Busse, R. & Nilius, B. (2005) *Circ. Res.* **97,** 908–915
15. Fernandez-Fernandez, J. M., Nobles, M., Currid, A., Vazquez, E. & Valverde, M. A. (2002) *Am. J. Physiol.* **283,** C1705–C1714
16. Jia, Y., Wang, X., Varty, L., Rizzo, C. A., Yang, R., Correll, C. C., Phelps, P. T., Egan, R. W. & Hey, J. A. (2004) *Am. J. Physiol.* **287,** L272–L278
17. Chung, M. K., Lee, H., Mizuno, A., Suzuki, M. & Caterina, M. J. (2004) *J. Biol. Chem.* **279,** 21569–21575
18. Alessandri-Haber, N., Yeh, J. J., Boyd, A. E., Parada, C. A., Chen, X., Reichling, D. B. & Levine, J. D. (2003) *Neuron* **39,** 497–511
19. Xu, F., Satoh, E. & Iijima, T. (2003) *Br. J. Pharmacol.* **140,** 413–421
20. Mosavi, L. K., Cammett, T. J., Desrosiers, D. C. & Peng, Z. Y. (2004) *Protein Sci.* **13,** 1435–1448
21. Gillo, B., Chorna, I., Cohen, H., Cook, B., Manistersky, I., Chorev, M., Arnon, A., Pollock, J. A., Selinger, Z. & Minke, B. (1996) *Proc. Natl. Acad. Sci. U. S. A.* **93,** 14146–14151
22. Niemeyer, B. A., Suzuki, E., Scott, K., Jalink, K. & Zuker, C. S. (1996) *Cell* **85,** 651–659
23. Xu, X. Z., Li, H. S., Guggino, W. B. & Montell, C. (1997) *Cell* **89,** 1155–1164
24. Erler, I., Hirnet, D., Wissenbach, U., Flockerzi, V. & Niemeyer, B. A. (2004) *J. Biol. Chem.* **279,** 34456–34463
25. Hellwig, N., Albrecht, N., Harteneck, C., Schultz, G. & Schaefer, M. (2005) *J. Cell Sci.* **118,** 917–928
26. Kedei, N., Szabo, T., Lile, J. D., Treanor, J. J., Olah, Z., Iadarola, M. J. & Blumberg, P. M. (2001) *J. Biol. Chem.* **276,** 28613–28619
27. Jahnel, R., Dreger, M., Gillen, C., Bender, O., Kurreck, J. & Hucho, F. (2001) *Eur. J. Biochem.* **268,** 5489–5496
28. Hoenderop, J. G., Nilius, B. & Bindels, R. J. (2003) *Pflugers Arch.* **446,** 304–308
29. Niemeyer, B. A. (2005) *Naunyn-Schmiedebergs Arch. Pharmacol.* **371,** 285–294
30. Schaefer, M. (2005) *Pflugers Arch.* **451,** 35–42
31. Balzer, M., Lintschinger, B. & Groschner, K. (1999) *Cardiovasc. Res.* **42,** 543–549
32. Engelke, M., Friedrich, O., Budde, P., Schafer, C., Niemann, U., Zitt, C., Jungling, E., Rocks, O., Luckhoff, A. & Frey, J. (2002) *FEBS Lett.* **523,** 193–199
33. Chang, Q., Gyftogianni, E., van de Graaf, S. F., Hoefs, S., Weidema, F. A., Bindels, R. J. & Hoenderop, J. G. (2004) *J. Biol. Chem.* **279,** 54304–54311
34. Garcia-Sanz, N., Fernandez-Carvajal, A., Morenilla-Palao, C., Planells-Cases, R., Fajardo-Sanchez, E., Fernandez-Ballester, G. & Ferrer-Montiel, A. (2004) *J. Neurosci.* **24,** 5307–5314
35. Amiri, H., Schultz, G. & Schaefer, M. (2003) *Cell Calcium* **33,** 463–470
36. Hamill, O. P., Marty, A., Neher, E., Sakmann, B. & Sigworth, J. (1981) *Pflugers Arch.* **391,** 85–100
37. Green, W. N. & Millar, N. S. (1995) *Trends Neurosci.* **18,** 280–287
38. Hurtley, S. M. & Helenius, A. (1989) *Annu. Rev. Cell Biol.* **5,** 277–307
39. Klausner, R. D., Donaldson, J. G. & Lippincott-Schwartz, J. (1992) *J. Cell Biol.* **116,** 1071–1080
40. Zerangue, N., Schwappach, B., Jan, Y. N. & Jan, L. Y. (1999) *Neuron* **22,** 537–548
41. Strubing, C., Krapivinsky, G., Krapivinsky, L. & Clapham, D. E. (2003) *J. Biol. Chem.* **278,** 39014–39019
42. Wang, C., Hu, H. Z., Colton, C. K., Wood, J. D. & Zhu, M. X. (2004) *J. Biol. Chem.* **279,** 37423–37430
43. Schulein, R. (2004) *Rev. Physiol. Biochem. Pharmacol.* **151,** 45–91
44. Schulteis, C. T., Nagaya, N. & Papazian, D. M. (1998) *J. Biol. Chem.* **273,** 26210–26217
45. Hermosilla, R. & Schulein, R. (2001) *Mol. Pharmacol.* **60,** 1031–1039
46. Jaskolski, F., Normand, E., Mulle, C. & Coussen, F. (2005) *J. Biol. Chem.* **280,** 22968–22976
47. Ellgaard, L., Molinari, M. & Helenius, A. (1999) *Science* **286,** 1882–1888
48. Ma, D. & Jan, L. Y. (2002) *Curr. Opin. Neurobiol.* **12,** 287–292
49. Watanabe, H., Vriens, J., Suh, S. H., Benham, C. D., Droogmans, G. & Nilius, B. (2002) *J. Biol. Chem.* **277,** 47044–47051
50. Black, D. L. (2003) *Annu. Rev. Biochem.* **72,** 291–336
51. Mery, L., Magnino, F., Schmidt, K., Krause, K. H. & Dufour, J. F. (2001) *FEBS Lett.* **487,** 377–383
52. Walker, R. L., Hume, J. R. & Horowitz, B. (2001) *Am. J. Physiol.* **280,** C1184–C1192
53. Schumacher, M. A., Moff, I., Sudanagunta, S. P. & Levine, J. D. (2000) *J. Biol. Chem.* **275,** 2756–2762
54. Oberwinkler, J., Lis, A., Giehl, K. M., Flockerzi, V. & Philipp, S. E. (2005) *J. Biol. Chem.* **280,** 22540–22548
55. Cohen, D. M. (2005) *Pflugers Arch.* **451,** 168–175
56. Stamm, S. (2002) *Hum. Mol. Genet.* **11,** 2409–2416